Life Sciences 232 (2019) 116603

Contents lists available at ScienceDirect

Life Sciences

journal homepage: www.elsevier.com/locate/lifescie

Trans-fatty acids aggravate anabolic steroid-induced metabolic disturbances and differential gene expression in muscle, pancreas and adipose tissue

Reggiani V. Gonçalves[a], Jamili D.B. Santos[b], Natanny S. Silva[b], Etienne Guillocheau[c], Robson E. Silva[d], Thaiany G. Souza-Silva[b], Rafael F. Oliveira[b,e], Eliziária C. Santos[f], Romulo D. Novaes[b,*]

[a] Department of Animal Biology, Federal University of Viçosa, 36570-000, Minas Gerais, Brazil
[b] Institute of Biomedical Sciences, Department of Structural Biology, Federal University of Alfenas, 37130-001, Minas Gerais, Brazil
[c] Laboratory of Biochemistry and Human Nutrition, Agrocampus-Ouest, 35042, Rennes, France
[d] School of Medicine, Federal University of Alfenas, 37130-001, Minas Gerais, Brazil
[e] School of Dentistry, Federal University of Alfenas, 37130-001, Minas Gerais, Brazil
[f] School of Medicine, Federal University of Jequitinhonha and Mucuri Valleys, 39100-000, Minas Gerais, Brazil

ARTICLE INFO

Keywords:
Experimental pathology
Glycemic control
Testosterone cypionate
Trans-fatty acids

ABSTRACT

Aims: Although anabolic steroids (AS) and trans-fatty acids overload exerts systemic toxicity and are independent risk factors for metabolic and cardiovascular disorders, their interaction remains poorly understood. Thus, we investigated the impact of a diet rich in trans-fatty acids (HFD) combined with AS on glycemic control, lipid profile, adipose tissue, skeletal muscle and pancreas microstructure and expression of genes involved in energy metabolism.

Main methods: Forty-eight C57BL/6 mice were randomized into 6 groups treated for 12 weeks with a standard diet (SD) or a diet rich in C18:1 trans-fatty isomers (HFD), alone or combined with 10 or 20 mg/kg testosterone cypionate (AS).

Key findings: Our results indicated that AS improved glycemic control, upregulated gene expression of *Glut-4* and *CPT-1* in skeletal muscle, *FAS*, *ACC* and *UCP-1* in adipose tissue. AS also reduced total and LDL cholesterol in mice fed a SD. When combined with the HFD, AS was unable to induce microstructural adaptations in adipose tissue, pancreatic islets and β-cells, but potentiated *GCK* and *Glut-2* (pancreas) and *Glut-4* and *CPT-1* (skeletal muscle) upregulation. HFD plus AS also downregulated *FAS* and *ACC* gene expression in adipose tissue. Combined with HFD, AS increased triacylglycerol circulating levels, improved insulin sensitivity and glycemic control in mice.

Significance: Our findings indicated that HFD and AS can interact to modulates glycemic control and lipid profile by a mechanism potentially related with a reprogramming of genes expression in organs such as the pancreas, adipose tissue and skeletal muscle.

1. Introduction

Dyslipidemias are metabolic disturbances with increasing incidence and prevalence worldwide [1,2]. These conditions have been closely correlated with several metabolic (*i.e.*, obesity, diabetes mellitus, and non-alcoholic fatty liver disease) and cardiovascular (*i.e.*, atherosclerosis, systemic arterial hypertension, myocardial infarction, and cardiac insufficiency) diseases, which are potentially preventable causes of death in general population [3,4]. Dyslipidemias exhibit a complex and multifactorial etiology, in which genetic determinants are central mediators of the lipid metabolism that orchestrate the pathophysiology of these diseases [5,6]. However, by acting as genetic modulators, environmental factors such as dietary habits and exposition to hormonal drugs are also implicated in dyslipidemias development [2,3].

Inadequate eating habits, with excessive ingestion of highly processed foods rich in carbohydrates and fats have been strongly implicated with the establishment of a low-grade and chronic pro-oxidant and pro-inflammatory status and the increased occurrence of a broad spectrum of metabolic diseases [7,8]. While dietary polyunsaturated

* Corresponding to: Rômulo Dias Novaes, Institute of Biomedical Sciences, Department of Structural Biology, Federal University of Alfenas, Rua Gabriel Monteiro da Silva 700, Alfenas, Minas Gerais, Brazil. Zip code: 37130-000. Phone/Fax: +55 35 3299-1300. E-mail address: romulo.novaes@unifal-mg.edu.br
E-mail address: romulo.novaes@unifal-mg.edu.br (R.D. Novaes).

https://doi.org/10.1016/j.lfs.2019.116603
Received 17 June 2019; Received in revised form 24 June 2019; Accepted 25 June 2019
Available online 27 June 2019
0024-3205/

fatty acids can be beneficial to control lipid metabolism and cardiovascular risk, excessive intake of saturated fatty acids has been associated with a pro-inflammatory status, marked insulin resistance, and increased incidence of dyslipidemia and non-alcoholic fatty liver disease (NAFLD) [9,10]. These effects are mediated by differential modulation of lipid-sensitive genes, including sterol regulatory element-binding proteins (SREBPs), acetyl-CoA carboxylase (ACC) and fatty acid synthase (FAS) [6,11,12]. Although gene modulation by polyunsaturated lipids is consistently characterized [11,12], the impact of trans-fatty acids on glucose metabolism pathways is still poorly understood [7].

Just like diets, steroid hormones exert a profound impact on energy metabolism [13]. This influence can be clearly observed throughout ageing and in cases of gonadal dysfunction and hormonal reposition, in which variations in hormone levels are often accompanied by changes in glucose homeostasis and lipid profile [14,15]. Anabolic steroids, especially testosterone analogues, were primarily developed for the treatment androgenic deficiencies, aplastic anaemia, growth disorders, and chronic diseases associated with cachexia [16]. However, these drugs have been used for aesthetic and athletic purposes to reduce fat mass, increase lean mass and athletic performance [14,17]. Due to the use of supraphysiological doses, hepatotoxicity, lipid profile disorders, atherosclerosis, heart failure and high mortality have been frequently reported in chronic users of these drugs [18,19]. There is evidence that by increasing the activity of hepatic triglyceride lipase, testosterone analogues reduce high-density [17,20] and increase low-density lipoproteins level, potentiating the risk of atherosclerosis and cardiovascular events [14].

Surprisingly, although high-fat diets (HFD) and anabolic steroids are independent risk factors for metabolic disorders, it is not yet understood if and how these factors can interact to modify organs structure, gene expression and energy metabolism. In a recent study, was reported that AS upregulates hepatic genes and determines a circulating and tissue lipid profile favourable to the development of NAFLD induced by HFD [21]. Considering a more comprehensive analysis of multiple organs involved in energy metabolism, we used a similar preclinical model to investigate the impact of a diet rich in trans-fatty acids and AS alone or combined on glycemic control, peripheral insulin resistance, lipid profile, microstructure and expression of genes involved in glucose and lipid metabolism in pancreas, adipose tissue, and skeletal muscle.

2. Material and methods

2.1. Animals, diets and treatments

Female 12 weeks-old C57BL/6 mice were kept in controlled environmental conditions (temperature 22 ± 2 °C, air humidity 60–70% and 12/12 h daily light/darkness cycles). The animals were randomized into 6 groups with 8 animals in each group. The groups fed a normolipidic diet received a standard diet (SD) alone or combined with the anabolic steroid testosterone cypionate at 10 mg/kg (SD + AS10) or 20 mg/kg (SD + AS20). The groups fed a hyperlipidic diet were treated with HFD alone or combined with testosterone cypionate at 10 mg/kg (HFD + AS10) or 20 mg/kg (HFD + AS20). Female animals were selected because of their low endogenous levels of androgenic steroids. Diet composition and energy values are presented in Table 1. Diet and water were provided *ad libitum* for 12 weeks. Diet intake, energy intake and body mass were weekly registered. Testosterone cypionate (Deposteron, EMS, Hortolandia, SP, Brazil) was administered by intraperitoneal injection every 48 h for 12 weeks. Testosterone doses were selected as they were effective in modulating hepatic gene expression and lipid metabolism in a previous study with female mice [21]. Twenty-four hours after the last treatment, the animals were euthanized by profound anaesthesia (250 mg/kg tribromoethanol, i.p.) and exsanguination. All visceral adipose tissue deposits (inguinal, periovarian, retroperitoneal, and mesenteric) were collected and weighed. The study was approved by the Institutional Ethics Committee on Animals Research (Protocol: 579/2014).

Table 1
Diet composition and profile of trans-fatty acids used in the experimental diet.

Composition (g/kg)	SD	HFD
Casein	140	70
Corn starch	560.7	206.7
Sucrose	100	50
Soy oil	100	–
Hydrogenated fat including (% of total fatty acids)	–	600
C18:1 5 *trans*	0	0.036205
C18:1 6–9 *trans*	0	10.09841
C18:1 10 *trans*	0	5.54772
C18:1 11 *trans*	0	4.720575
C18:1 12 *trans*	0	3.272375
C18:1 13 *trans*	0	2.10546
C18:1 14 *trans*	0	1.306165
C18:1 15 *trans*	0	0.50687
C18:1 16 *trans*	0	0.259005
Total fibers	50	25
Vitamin mix	10	10
Mineral mix	35	35
L-Cysteine	1.8	1.8
Choline	2.5	2.5
Total (g)	1000	1000
Energy (kcal/kg)	3713	5802
Carbohydrate (%)	71	28
Protein (%)	14	7
Lipid (%)	10	60

SD, standard diet; HFD, high-fat diet.

2.2. Characterization of dietary trans-fatty acids by gas chromatography

As the HFD contained partially hydrogenated vegetable oil (PHVO), detailed analysis of *trans*-fatty acids was carried out. To remove impurities, lipids from the PHVO were extracted using chloroform/methanol [22]. Lipids were derivatized as fatty acids methyl esters (FAME) according to a two-step procedure using NaOH (0.5 M in methanol) and BF_3 [23]. FAMEs were then extracted twice with pentane and NaCl (0.9%). $AgNO_3$-thin layer chromatography was subsequently performed to separate *cis* and *trans*-FAME as previously described [24]. Finally, *trans*-FAME were analyzed with an Agilent 7890 N gas chromatograph (Agilent Technologies, Santa Clara, CA, USA) equipped with a bonded fused silica capillary column (BPX90; 100 m × 0.25 mm, 0.25 μm thickness; SGE Analytical Science, Melbourne, Australia). The temperature program started at 120 °C for 120 min, then increased to 260 °C at 10 °C/min and held for 10 min. Helium was used as carrier gas. Mass spectra were recorded with an Agilent 5975C MSD (Agilent Technologies). The mass spectrometer was operated under electron impact ionization conditions (electron energy 70 eV, source temperature 230 °C). Data were obtained in full-scan mode with a mass range of *m/z* 50–550 amu. Identification of peaks relied on previously published analysis of PHVOs [25]. Peak integration was accomplished with MassHunter Workstation Software, Qualitative Analysis, version B.07.00 (Agilent Technologies).

2.3. Plasmatic triacylglycerol and cholesterol levels

Triacylglycerol, total cholesterol, LDL and HDL cholesterol levels were quantified in plasma by spectrophotometer by using commercial kits and the instructions provided by the manufacturer (Bioclin, Belo Horizonte, Minas Gerais, Brazil) [26].

2.4. Glucose and insulin tolerance tests

The oral glucose tolerance test (OGTT) was performed with all

Table 2
Dietary intake and body mass in control mice and those treated with high-fat diet and anabolic steroid.

Parameters	Initial body mass (g)	Final body mass (g)	Visceral fat (g)	Diet intake (g/g mass/day)	Energy intake (kj/g mass/day)
SD	20.55 ± 2.57[a]	29.11 ± 1.41[a]	3.01 ± 0.56[a]	0.25 ± 0.09[a]	3.88 ± 1.40[a]
SD + AS10	20.90 ± 2.66[a]	28.72 ± 1.62[a]	3.08 ± 0.44[a]	0.27 ± 0.07[a]	4.19 ± 1.09[a]
SD + AS20	19.11 ± 1.73[a]	32.95 ± 2.34[b]	2.93 ± 0.51[a]	0.31 ± 0.08[a]	4.81 ± 1.24[a,b]
HFD	19.70 ± 2.60[a]	28.23 ± 2.50[a]	3.17 ± 0.60[a]	0.26 ± 0.05[a]	6.31 ± 1.21[b,c]
HFD + AS10	20.15 ± 2.52[a]	28.15 ± 1.55[a]	3.05 ± 0.53[a]	0.29 ± 0.08[a]	7.04 ± 1.94[c]
HFD + AS20	20.63 ± 1.70[a]	29.27 ± 2.40[a]	2.98 ± 0.49[a]	0.27 ± 0.06[a]	6.55 ± 1.50[c]

SD = standard diet, HFD = high-fat diet, AS10 and 20 = anabolic steroid testosterone cypionate administered at 10 and 20 mg/kg. [a, b, c]Different letters in the columns indicate statistical difference between groups ($P < 0.05$), and groups with the same letter are statistically similar ($P > 0.05$).

Table 3
Plasma biochemical parameters in control mice and those treated with high-fat diet and anabolic steroid.

Groups/parameters	Glucose (mmol/L)	Insulin (pmol/L)	HOMA-IR index
SD	10.25 ± 0.91[a]	150.69 ± 5.63[a]	68.57 ± 4.98[a]
SD + AS10	10.16 ± 0.56[a]	149.64 ± 2.93[a]	67.52 ± 3.49[a]
SD+ AS20	9.59 ± 0.85[a]	135.25 ± 3.90[b]	54.17 ± 5.00[b]
HFD	7.24 ± 0.62[b]	130.59 ± 4.48[b]	49.23 ± 4.24[b]
HFD + AS10	7.48 ± 0.62[b]	119.25 ± 1.84[c]	39.66 ± 3.57[c]
HFD + AS20	7.74 ± 0.79[b]	112.67 ± 2.06[d]	38.77 ± 3.92[c]

HOMA-IR = homeostasis model assessment of insulin resistance, SD = standard diet, HFD = high-fat diet, AS10 and 20 = anabolic steroid testosterone cypionate administered at 10 and 20 mg/kg. [a, b, c, d]Different letters in the lines indicate statistical difference between groups ($P < 0.05$), and groups with the same letter are statistically similar ($P > 0.05$).

animals fasted for 16 h, without water restriction. Then, anhydrous glucose (3 g/kg of body weight) diluted in 1 mL of distilled water (*w/v*) was administered by gavage. Blood samples were collected by tail vein puncture at 0 (fasting glucose), 30, 60, 90 and 120 min and blood glucose was measured by a glucose oxidase method (OneTouch Ultra, Jonson & Jonson, CA, USA). The area under the blood glucose response curve (AUC) was calculated for each animal using the trapezoidal method [27].

Insulin tolerance test (ITT) was performed 48 h after OGTT, with all animals fasted for 2 h. The animals were injected subcutaneously at the back of the neck with 0.5 units/kg insulin (Biochemica, Florida, USA) and the blood glucose measured at 0, 30, 60, 90 and 120 min. by the same glucose oxidase method. The ratio of glucose decayment constant (KITT) was calculated using the relation 0.693/(T1/2), where T1/2 of plasmatic glucose was determined through the inclination of the glucose curve during its phase of linear decayment (0–30 min) [28].

2.5. Blood glucose and insulin resistance

Blood glucose was measured by a glucose oxidase method using a handheld glucometer (Accutrend Plus, Roche, WI, USA). Plasma insulin levels were determined by Enzyme-Linked Immunosorbent Assay (ELISA) by using a commercial kit and the instructions provided by the manufacturer (Cayman Chemical, Ann Arbor, MI, USA). The homeostasis model assessment of insulin resistance (HOMA-IR) was calculated as (insulin [mU/l] × glucose [mmol/l]) / 22.5 to assess insulin resistance. All parameters were measured after 6 h of fasting [29].

2.6. Pancreas microstructure and β-cells histochemistry

The pancreas samples were fixed in 10% paraformaldehyde for 48 h at room temperature. After inclusion in paraffin, sections with 4-μm thickness were obtained with a 200 μm interval to avoid evaluating the same histological field. The sections were stained with an aldehyde-fuchsine histochemical method for β-cells [28]. The number of pancreatic islets and β-cells was directly counted from 100 random non-coincident histological fields obtained with a magnification of 50× (total area = $3.08 \times 10^5\ \mu m^2$) and 400× (total area = $3.85 \times 10^4\ \mu m^2$), respectively. The total tissue area and islet area were directly measured using a computational contour function [28]. The number density of pancreatic islets per histological area (n/mm^2) and β-cells per islet area (cells/m^2) were estimated by dividing the number of pancreatic islets by the total tissue area, and β-cells number by the islet cross-sectional area, respectively. The proportion of β-cells was estimated as the mean values obtained by two computational method based on RGB histogram [30,31] and colour segmentation function [32]. The volume (V) of pancreatic islets was estimated by the prolate (P) spheroid method according to the formula $VP = (4/3) * \pi a^2 b$; where a is the equatorial (minor) radius *a* and *b* is the polar (major) radius of the islet cross-sectional profile [33]. The Image Pro-Plus 4.5 (Media Cybernetcs, Silver Spring, MD, USA) and ImageJ [32] image analysis software were used in all quantifications [28].

2.7. Adipose tissue and skeletal muscle microstructure

Mesenteric adipose tissue and skeletal muscle (tibialis anterior) samples were fixed in 10% paraformaldehyde for 48 h at room temperature. After inclusion in 2-hydroxyethyl methacrylate resin, sections with 3-μm thickness were obtained with a 200-μm interval to avoid evaluating the same histological field. Skeletal muscle was stained with toluidine blue and basic fuchsine, while adipose tissue sections were stained with toluidine blue alone. The slides were mounted and digital images were obtained using a bright field photomicroscope (AxionVision A1, Carl Zeiss, Germany). The number of histological fields used to analyze tissue microstructure was based on the method of stabilization of the coefficient of variation [28]. Thus, 100 random non-coincident histological fields in each group and tissue were randomly obtained and analyzed with a × 40 objective lens, in a total test area (At) of $3.64 \times 10^5\ \mu m^2$. The morphological analysis was performed using the Image Pro-plus 4.5 software (Media Cybernetcs, Silver Spring, MD, USA) [34].

2.8. Adipose tissue and skeletal muscle stereology

The stereological method was used in the microstructural analysis of adipose tissue and skeletal muscle. In this method, a 200-points (P_T) test system was applied in a standard test area (A_T) of $73 \times 10^3\ \mu m^2$ [35,36]. The volume density (Vv, %) occupied by skeletal myocytes (MI) and connective tissue (CT) was estimated as $Vv = P_P/P_T$; where P_P is the number of points hitting MI or CT [34]. The number density (Q_A) of unilocular adipocytes (AP) was estimated as $Q_{A\ AP} = \Sigma AP/A_T$; where IC is the number of interstitial cells and AP is the number of adipocytes counted in the test area. The area of adipocytes was directly measured from a contour function. The diameter of skeletal myocytes was determined by linear planimetry. The image analysis software Image Pro-plus 4.5 (Media Cybernetcs, Silver Spring, USA) was used in all analysis [34].

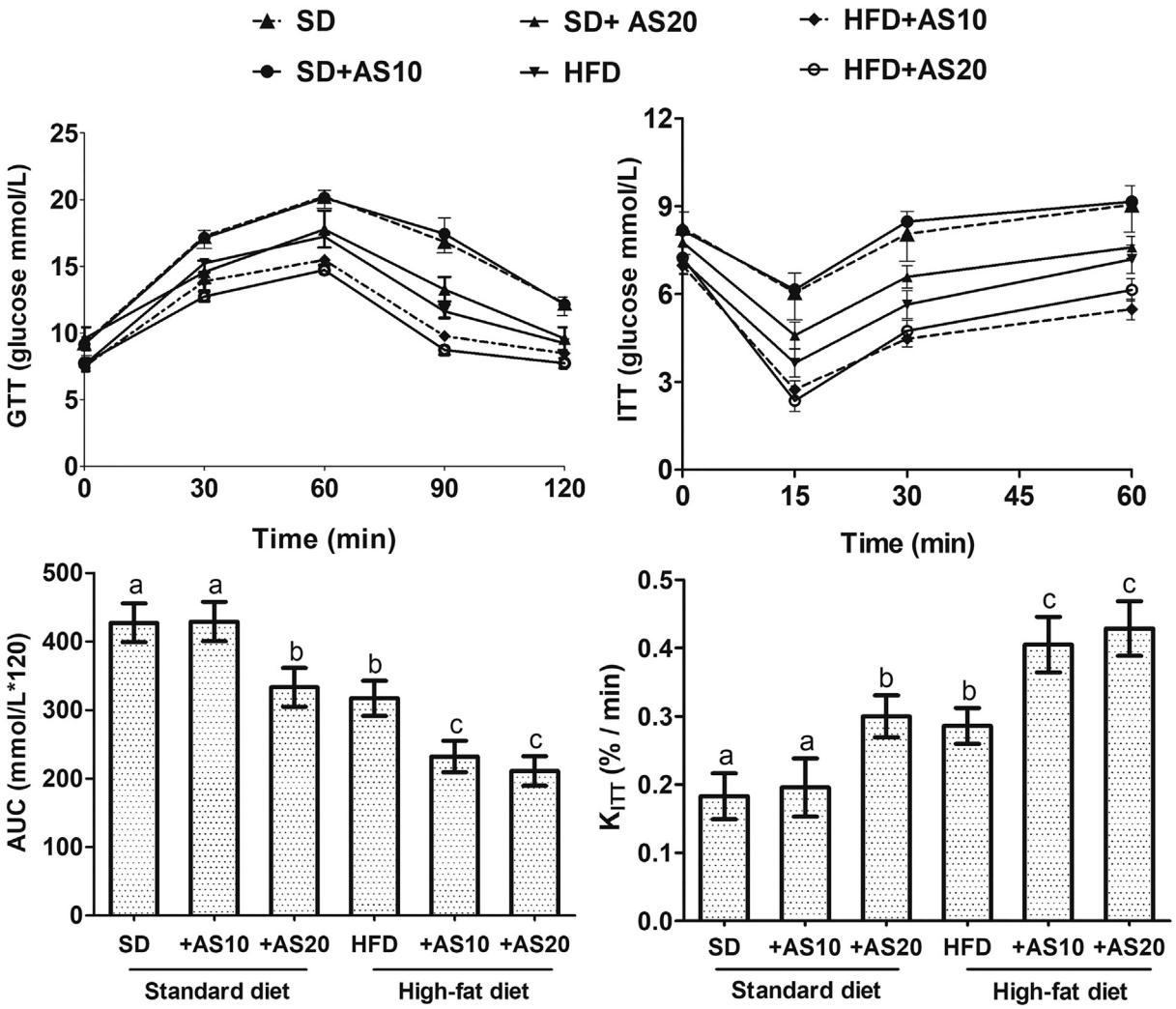

Fig. 1. Glucose tolerance and insulin tolerance tests in mice treated with standard diet (SD) or high-fat diet (HFD) and the anabolic steroid (AS) testosterone cypionate. GTT = glucose tolerance test, ITT = insulin tolerance test, AUC = area under the glucose curve in GTT, K_{ITT} = glucose decay rate in ITT, AS10 and 20 = anabolic steroid testosterone cypionate administered at 10 and 20 mg/kg. Different letters (a,b,c) in the columns denote statistical differences among the groups ($P < 0.05$), and groups with the same letter are statistically similar ($P > 0.05$).

2.9. Gene expression in pancreas, adipose tissue and skeletal muscle

Acetyl-CoA carboxylase (*ACC*), fatty acid synthase (*FAS*), and uncoupling protein 1 (*UCP-1*) gene expression was determined in brown adipose tissue (BAT - collected in the interscapular area). Glucokinase (*GCK*) and glucose transporter 2 (*Glut-2*) expression were evaluated in the pancreas. Glucose transporter 4 (*Glut-4*) and carnitine palmitoyltransferase 1 (*CPT-1*) mRNA expression were analyzed in skeletal muscle (tibialis anterior). The expression of all target genes was evaluated by real-time quantitative PCR (qRT-PCR) according to Yessoufou et al. [37]. Briefly, cDNA was obtained using a commercial reverse transcription kit (ThermoFisher Scientific Waltham, MA, USA) and the manufacturer's instructions. All primers used were previously validated [37–41]: *FAS* forward 5′-AGTGTCCACCAACAAGCG-3′, reverse 5′-GATGCCGTCAGGTTTCAG-3′; *ACC* forward 5′-CCACACTGAACCGGAAATCT-3′, reverse: 5′-ATTTGTCGTAGTGGCCGTTC-3′; *GCK* forward 5′-AGAAGGCTCAGAAGTTGGAGAC-3′, reverse 5′-GGATGGAATACATCTGGTGTTTCG-3′; *Glut-2* forward 5′-TGTGGTGTCGCTGTTTGTTG-3′, reverse 5′-AATGAAGTTTGAGGTCCAGTTGG-3′; *Glut-4* forward 5′-AAAAGTGCCTGAAACCAGAG-3′, reverse 5′-TCACCTCCTGCTCTAAAAGG-3′; *CPT-1* forward 5′-TCTTGCAGTCGACTCACCTT-3′, reverse 5′-TCCACAGGACACATAGTCAGG-3′; and *GAPDH* forward 5′-TGCGACTTCAACAGCAACTC-3′, reverse 5′-GCCTCTCTTGCTCAGTGTCC-3′. qPCR reactions used SYBR Green PCR Mastermix (Applied Biosystems, Carlsbad, CA, USA) and the manufacturer's instructions. The relative mRNA expression was determined using the ΔΔCt method, in which ΔΔCt = ΔCt of the target gene − ΔCt of *GAPDH*. ΔCt = Ct of group of interest − Ct of the control group. Relative quantity (RQ) was calculated as $RQ = (1 + E)(-\Delta\Delta Ct)$.

2.10. Statistical analysis

Results were expressed as mean and standard deviation (mean ± SD) or median and interquartile intervals. Data distribution was evaluated by D'agostino-Pearson test. Data with normal distribution were submitted to two-way analysis of variance (two-way ANOVA) followed by Student-Newman-Keuls (SNK) *post hoc* test. Nonparametric data were compared by Kruskal-Wallis test. A P value ≤ 0.05 indicated a statistical difference in all tests.

3. Results

Diet composition of the experimental diets is detailed in Table 1. Nine C18:1 trans isomers were identified in HFD, which are usually found in partially hydrogenated oils commercially available.

All groups presented similar initial body mass, visceral fat mass and

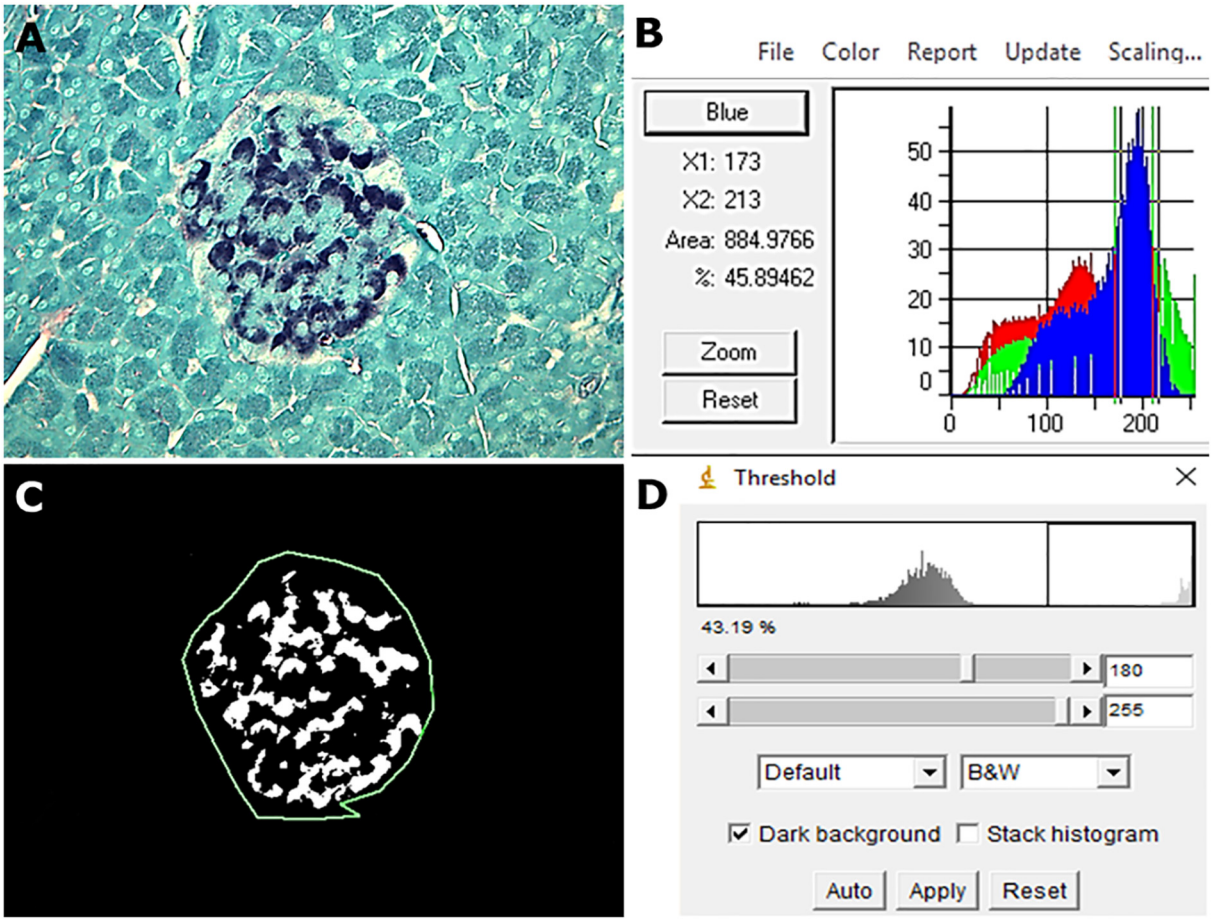

Fig. 2. Quantification of β-cells marked in pancreatic islets by insulin histochemistry in mice treated with standard diet or high-fat diet and the anabolic steroid testosterone cypionate. (A) Microscopic image of the pancreas with a Langerhans islet in a central position and β-cells marked in dark blue colour. (B) Analysis of β-cells distribution by RGB colour histogram on Image-Pro Plus image processing software. (C) Background removal by black and white segmentation on ImageJ image processing software. (D) Delimitation of islet area and confirmation of β-cells area by image segmentation. (For interpretation of the references to colour in this figure legend, the reader is referred to the web version of this article.)

Table 4
Microstructural pancreatic parameters in control mice and those treated with high-fat diet and anabolic steroid.

Groups/parameters	Islets (n/mm^2)	Islets (μm^3) × 10^6	β-Cell (n/mm^2)	β-Cell (%/islet area)
SD	0.83 ± 0.25^a	2.27 ± 0.40^a	10,413 ± 4579^a	45.98 ± 15.31^a
SD + AS10	0.90 ± 0.36^a	2.35 ± 0.48^a	11,559 ± 5123^a	49.63 ± 16.28^a
SD + AS20	0.85 ± 0.29^a	2.61 ± 0.41^a	10,601 ± 5927^a	47.39 ± 16.83^a
HFD	0.94 ± 0.47^a	2.68 ± 0.55^a	12,328 ± 4833^a	50.02 ± 14.55^a
HFD + AS10	0.90 ± 0.52^a	2.71 ± 0.57^a	12,916 ± 6141^a	52.19 ± 15.62^a
HFD + AS20	0.88 ± 0.40^a	2.79 ± 0.62^a	12,159 ± 5611^a	50.27 ± 17.01^a

SD = standard diet, HFD = high-fat diet, AS10 and 20 = anabolic steroid testosterone cypionate administered at 10 and 20 mg/kg. The same letter (a) in the columns indicate that the groups are statistically similar (P > 0.05).

diet intake ($P > 0.05$). Final body mass was higher in the group SD + AS20 compared to the other groups ($P < 0.05$). Energy intake was similar in the groups SD, SD + AS10, and SD + AS20 ($P > 0.05$), but higher in the groups HFD, HFD + AS10 and HFD + AS20 ($P < 0.05$), Table 2.

The group SD + AS20 exhibited similar plasma glucose levels but reduced insulin and HOMA-IR index compared to the groups SD and SD + AS10 (P > 0.05). Animals concomitantly treated with HFD, especially those receiving AS, had a marked reduction in glucose and insulin plasma levels, and HOMA-IR index compared to the other groups ($P < 0.05$), Table 3.

Glucose kinetics in GTT and ITT was changed in the group SD + AS20 and all groups treated with HDF (Fig. 1). In GTT, the increase in blood glucose was less pronounced and the area under the glucose curve was reduced in the group SD + AS20 and in animals receiving the HFD, especially in combination with AS ($P < 0.05$). Conversely, these animals exhibited rapid and pronounced blood glucose decay rate (K_{ITT}) in ITT and compared to all the groups SD and SD + A10 (P < 0.05).

Pancreatic islets were analyzed and β-cells were quantified from a computational method detailed in Fig. 2. From the histochemical method, pancreatic islets were well-defined and β-cells exhibited a high resolution, which was required for the quantitative analysis. The microstructural quantitative analysis indicated that the number and volume of pancreatic islets, as well as the number and distribution of β-Cell in pancreatic islets, was similar in all groups ($P > 0.05$), Table 4.

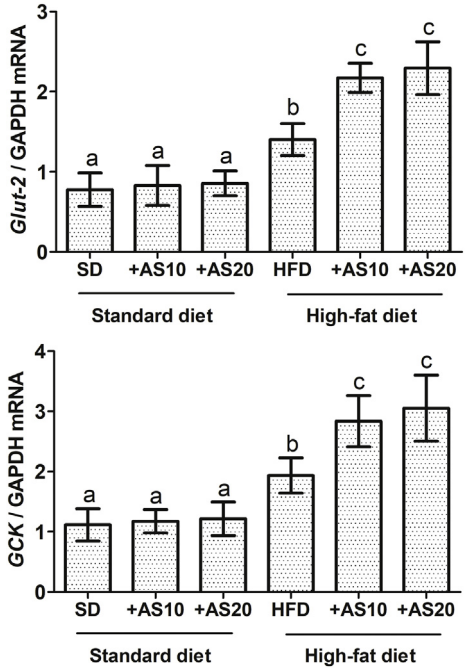

Fig. 3. Gene expression in the pancreas of mice treated with standard diet (SD) or high-fat diet (HFD) and the anabolic steroid (AS) testosterone cypionate. ACC = acetyl-CoA carboxylase, FAS = fatty acids synthase, Glut-2 = glucose transporter 2, GCK = glucokinase, AS10 and 20 = testosterone cypionate administered at 10 and 20 mg/kg. Different letters (a, b, c) in the columns denote statistical differences among the groups ($P < 0.05$), and groups with the same letter are statistically similar ($P > 0.05$).

In the pancreas, *Glut-2* and *GCK* gene expression was increased in all groups treated with HFD, especially HFD + AS10 and HFD + AS20 compared to the other groups ($P < 0.05$). These genes presented similar expression in the groups treated with SD alone or combined with AS ($P > 0.05$), Fig. 3.

The microscopic examination indicated a well-organized muscular structure in all groups analyzed, in which were observed well-delimited skeletal myocytes and reduced interstitial cellularity. Muscle mass, parenchymal distribution and myocytes diameter were increased in the groups SD + AS20 compared to the other groups ($P < 0.05$), which exhibited similar morphological parameters ($P > 0.05$), Fig. 4.

In skeletal muscle, *Glut-4* and *CPT-1* gene expression were similarly increased in the groups SD + AS20 and HFD, and even more upregulated in HFD + AS10 and HFD + AS20 compared to the other groups ($P < 0.05$), Fig. 5.

The groups HFD, and especially HFD + AS10 and HFD + AS20 exhibited increased triacylglycerol and reduced HDL cholesterol plasma levels compared to the other groups ($P < 0.05$), which were similar between them ($P > 0.05$). Total cholesterol was reduced in the group SD + AS20 compared to the other groups ($P < 0.05$). LDL cholesterol was reduced in the groups SD + AS10 and SD + AS20 compared to the other groups ($P < 0.05$), Table 5.

Morphological analysis of adipose tissue is shown in Fig. 6. The number and area of adipocytes were similar in all groups investigated ($P > 0.05$).

Compared with the groups SD and SD + AS10, *FAS* and *ACC* gene expression in white adipose issue were increased in the group SD + AS20 ($P < 0.05$) and reduced in all groups receiving the HFD, especially those concomitantly treated with AS ($P < 0.05$). In brown adipose tissue, animals in the groups SD + AS10, SD + AS20 and HFD exhibited increased *UCP-1* gene expression compared the group SD ($P < 0.05$). This gene was even more upregulated in the groups HFD + AS20 and HFD + AS10 compared to the other groups ($P < 0.05$). (See Fig. 7.)

4. Discussion

Considering that HFD and AS are isolated risk factors for metabolic diseases, it is surprising that the interaction between them is systematically neglected and poorly understood. For the first time, we observed clear evidence that HFD and AS combined exerts a profound influence on lipid and glucose metabolism in multiple organs. Our findings indicated that HFD and AS treatment was not associated with microstructural adaptations in the pancreas and adipose tissue, but induced mild remodelling in skeletal muscle. Only animals treated with SD combined with the highest dose of AS exhibited increased body mass. As diet and energy intake were similar or increased in the other groups, our findings were consistent with a dose-dependent effect of AS on feed efficiency in animals receiving the SD. However, this effect was not observed in mice treated with HFD, indicating that diet composition exerts a central role on the anabolic effect of AS. Despite the higher lipid and energy content, adjusted protein levels are essential to support general body growth [42,43]. There is evidence that in response to protein deficiency occurs a metabolic deviation of amino acids to ensure the homeostatic function of vital organs (*e.g.*, brain, heart, and liver), at expense of reduced body growth [42,43]. As protein synthesis is the main effect of AS [16,44], it is not surprising that unbalanced diets block the anabolic effect in animals treated with testosterone cypionate. As all groups exhibited similar visceral fat mass and microstructural characteristics of the adipose tissue, the general body growth was independent of visceral fat accumulation in the group SD + AS20, and potentially related to increased lean mass.

Beyond the impact on body growth, HFD and AS alone and especially combined exerted a profound impact on glycemic control. Thus, key genes involved in energy metabolism in the pancreas, skeletal muscle and adipose tissue were investigated. Glut-4 is involved in glycemic control by acting as insulin-dependent glucose transporter highly expressed in cardiac and skeletal myocytes. Glut-4 participates of the cellular metabolic control, and its increased expression is associated with intense glycolytic or oxidative pathways responsible for energy generation and improved insulin sensitivity [45,46]. By transfer long-chain fatty acids into the mitochondria, CPT-1 plays an important role in energy metabolism by stimulating β-oxidation [47,48]. Due to malonyl-CoA accumulation, physiological hyperglycemia and hyperinsulinemia inhibit CPT-1 and fat oxidation. Thus, fatty acids in excess are esterified determining increased triacylglycerol accumulation in skeletal muscles, which is associated with increased insulin resistance [47]. In addition, UCP-1 is highly produced in BAT and is directly involved in energy metabolism by uncoupling oxidative phosphorylation to produce heat instead of chemical energy (ATP) [49]. There is evidence that the higher UCP-1 levels are associated with a protective phenotype against diabetes and obesity [49,50]. BAT is an insulin-sensitive tissue that beyond glucose, also use fatty acids for thermogenesis, indicating a regulatory role of this tissue on body adiposity, glucose homeostasis and insulin sensitivity in animals and humans [50].

From similar microstructural characteristics in all groups, morphological abnormalities in pancreatic islets were unable to explain the changes in glycemic control induced by AS in HFD-treated mice. However, animals treated with HFD alone also exhibited increased *Glut-2* and *GCK* gene expression in pancreas, especially when combined with AS. Thus, it is possible that together with *Glut-4*, *CPT-1* and *UCP-1* gene expression, *Glut-2* and *GCK* genes in pancreas are additionally activated to improve the glycemic control in animals treated with HFD, a mechanism potentially reinforced by AS that requires further investigation. Glut-2 is a facilitated diffusion glucose transporter highly expressed in the plasma membrane of pancreatic β-cells in animals and humans [51,52]. This transporter regulates cellular glucose uptake and its inactivation suppresses glucose-mediated insulin secretion (GMIS) in

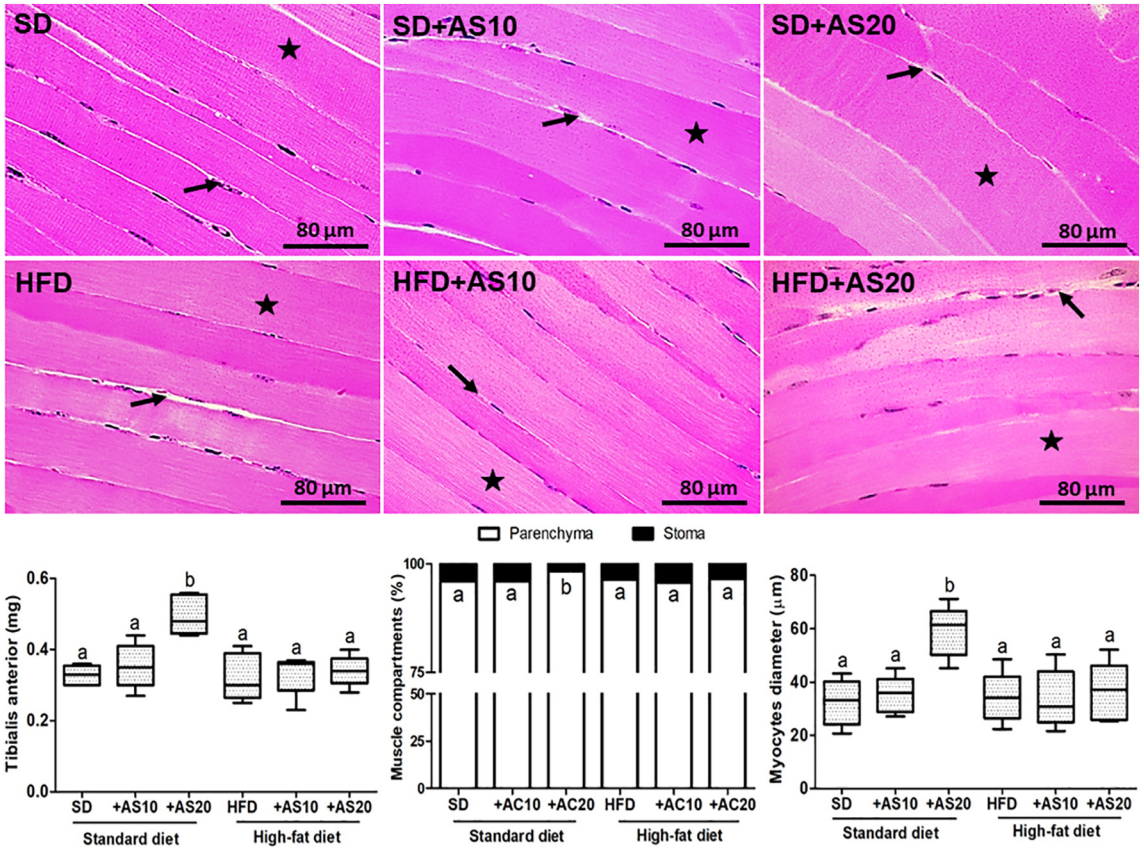

Fig. 4. Representative photomicrographys and microstructural quantitative parameters in skeletal muscle of mice treated with standard diet (SD) or high-fat diet (HFD) and the anabolic steroid (AS) testosterone cypionate. AS10 and 20 = testosterone cypionate administered at 10 and 20 mg/kg. In the images: Stars = skeletal myocytes (parenchyma), Arrows = connective tissue (stroma). In the graphics, different letters (a, b) in the columns denotes statistical differences among the groups ($P < 0.05$), and groups with the same letter are statistically similar ($P > 0.05$).

rodent pancreas, determining early postnatal death in mice [51,52]. Glucose uptake by Glut-2 is required as the first step in the metabolic signalling pathway that regulates GMIS, which is also dependent on GCK [52]. GCK is a low-affinity glucose-phosphorylating enzyme expressed in pancreatic *β*-cells and hepatocytes. In *β*-cells, GCK acts as a signal-recognizing enzyme sensitive to small variations in blood glucose, determining glucose phosphorylation and glycolysis activation, increasing ATP/ADP ratio, as well as the activation of ATP-sensitive K^+ and Ca^{2+} channels, which triggers the insulin granules exocytosis [51,52].

In a previous study, Kim et al. [53] reported that rats treated with an isocaloric HFD for 10 weeks exhibited 50% reduction in insulin plasma levels, *Glut-2* and *GCK* mRNA, suggesting impaired signal transduction mechanism in pancreatic β-cells compared with animals receiving a high-carbohydrate diet. However, Reimer and Ahrén [54] showed that even in the absence of morphological adaptations in pancreatic islets and *β*-cell, 8 weeks of HFD were enough to increase GMIS, indicating a functional compensatory mechanism not observed 1 an 4 weeks of dietary intervention. Winzell et al. [55] also reported impaired insulin response 1 week after administration of a 30% fat diet, which was adaptively improved after 16 weeks. Considering the same principle applied in our model, Kennedy et al. [56] also indicated that mice eating a low-carbohydrate/HFD failed to gain body mass, despite the high energy density of the diet. In this study, these animals also exhibited reduced insulin plasma levels and improved glucose tolerance, a finding attributed to changes in *Glut-2* and *GCK* gene expression.

Divergent results of gene expression and glycemic control have been reported following the exposition to HFD [53,55]. Kim et al. [57] indicated that short-term HFD feeding reduced *Glut-4* gene expression and impaired glucose metabolism in C57BL/6 mice. However, long-term HFD reduced glucose and insulin plasma levels and improved the glycemic control, which was correlated with an adaptive increase of *Glut-4* gene expression. In addition, while high glycemic load and glucose oxidation is related to reduced CPT-1 levels, fasting stimulates CPT-1 production and activity, improving fat oxidation and insulin sensitivity in animals and humans [58]. As the malonyl CoA content of rat skeletal muscle increases with carbohydrate intake, low-carbohydrate HFD is effective to increases *β*-oxidation, with an effect potentially mediated by the increased CPT-1 production and activity [58]. Although detailed mechanism by which CPT-1 modulates glucose metabolism is poorly understood, it has been suggested that long-chain fatty acyl-CoA and its conversion in diacylglycerol might modulate the activity of protein kinase C and phosphatidylinositol 3-kinase, impairing the phosphorylation of insulin receptor substrate 1 (IRS-1), Glut-4 translocation to cell membrane and the insulin signalling cascade [48]. Conversely, due its central role in stimulating *β*-oxidation [58] increased *CPT-1* muscle expression was expected in HFD-treated animals, representing an adaptive mechanism in response to high lipid loads, which was also observed by Collino et al. [59] in mice treated for 12 weeks with HFD. Although a similar response was be induced by the steroid alone, the combination with HFD enhanced *CPT-1* gene expression, indicating a complex interaction in the modulation of muscle energy metabolism that requires further clarification.

In addition to the impact of HFD on energy metabolism, the highest dose of AS improved glycemic control by reducing insulin resistance in SD-treated animals. AS also potentiated insulin sensitivity already observed in mice treated with HFD alone. Reduced insulin resistance was not surprising in animals receiving a low-carbohydrate HFD, especially considering that increased expression and sensitivity of insulin receptors in peripheral tissues are a typical metabolic adjustment to

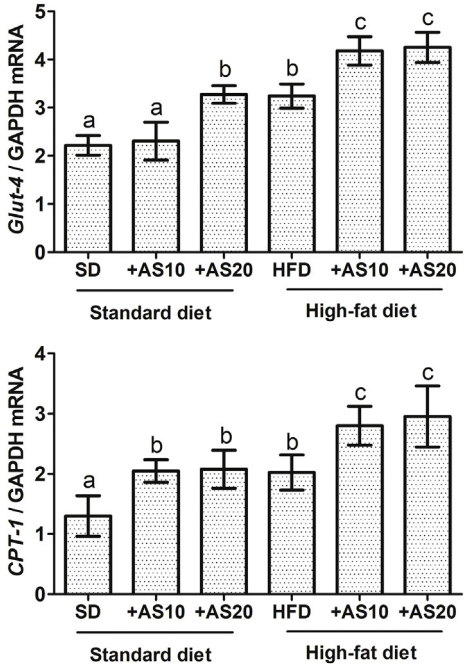

Fig. 5. Gene expression in skeletal muscle of mice treated with standard diet (SD) or high-fat diet (HFD) and the anabolic steroid (AS) testosterone cypionate. Glut-4 = glucose transporter 4, CPT-1 = carnitine palmitoyltransferase 1, AS10 and 20 = testosterone cypionate administered at 10 and 20 mg/kg. Different letters (a, b, c) in the columns denote statistical differences among the groups ($P < 0.05$), and groups with the same letter are statistically similar ($P > 0.05$).

improve glucose uptake [57]. In this sense, reduced insulin plasma levels detected were also consistent with increased *Glut-4* and *CPT-1* gene expression in skeletal muscle and *UCP-1* expression in brown adipose tissue, indicating that AS can modulate insulin resistance and glucose metabolism in animals treated with SD and HFD. This effect was clearly observed from glucose and insulin tolerance tests, in which animals treated with HDF and AS combined showed more efficient and faster glycemic control than animals treated with SD or HFD alone. As *Glut-2* and *GCK* gene expression was unaffected in the pancreas of animals treated with SD alone or combined with AS, the improved glycemic control in AS-treated animals was potentially related to the increased gene expression in skeletal muscle and adipose tissue.

As a systematically neglected issue, the impact of AS alone and especially combined with HFD on gene expression and carbohydrate metabolism remains poorly understood. Therefore, our findings on glucose metabolism were interpreted considering an interaction between diet and steroid hormones with similar chemical properties, especially sexual hormones. In this sense, increased expression and synthesis of *Glut-4* was reported rat cardiac myocytes treated with testosterone, indicating that *Glut-4* in directed involved in the improved glucose uptake induced by androgen [60]. High levels of steroid hormones such as estradiol and progesterone are also associated with increased insulin gene expression, GCK activity and insulin plasma levels [61]. Conversely, reduced levels in these hormones attenuate *K ATP* gene expression and GMIS in pancreatic islets. Apparently, this response is mediated by the modulatory effect of sex hormones on *Pdx1* and *Irs2* genes, which are involved in *β*-cell maturation by acting as modulators of tyrosine kinase receptors and transcription factor for the insulin promoter gene [61]. By decrease NF-$_K$B nuclear translocation, mitochondrial cytochrome *c* release and caspase 9 activation, estrogens also exert a cytoprotective effect on pancreatic islets, downregulating apoptotic pathways in *β*-cells [62]. *In vitro* and *in vivo* evidence also indicated that mice lacking androgen receptors in *β*-cells exhibits decreased GMIS and glucose intolerance [63]. In this study, while testosterone increased insulin gene expression in pancreas, hormonal depletion by gonadectomy downregulated insulin mRNA and plasma levels. Beyond exerting a protective effect against the development of diabetes in female non-obese diabetic mice [61], the treatment with dehydroepiandrosterone also increases *β*-cells mass and GMIS in pancreatic islets from aged rats [64]. It has been suggested that this effect is partially mediated by hormone-induced cAMP biosynthesis, protein kinase A and glucagon-like peptide-1 receptor activation in pancreatic islets, improving the glycemic control in type 2 diabetes and hypogonadal men [63,65].

Together with the marked impact on glycemic control, AS reduced total cholesterol and LDL levels in SD-treated animals, while increasing blood triacylglycerol and reducing HDL cholesterol in HFD-treated mice. This impact on lipid profile was dissociated from microstructural changes in adipocytes but was potentially associated with *FAS* and *ACC* gene expression in adipose tissue. Apparently, the upregulation of these lipogenic genes [66,67] was not associated with elevation of circulating lipid levels in SD-treated mice. Conversely, *FAS* and *ACC* genes were interestingly downregulated in response to HFD alone and especially when combined with AS, reinforcing our hypothesis that the dyslipidemia observed in our study was a result of dietary lipid accumulation rather than *de novo* fatty acids biosynthesis. Considering that diet and *de novo* lipogenesis are the two sources of fatty acids [67], it was expected that endogenous lipogenic pathways are inhibited by HFD. *FAS* gene and its encoded enzyme are central lipogenic regulators, catalyzing the last step of fatty acids biosynthesis from acetyl-CoA, malonyl-CoA and NADPH [67]. The enzyme ACC (especially the isoform ACC1) is also involved in *de novo* lipogenesis, catalyzing the synthesis of malonyl-CoA [66]. As the isoform ACC2 exerts inhibitory effects on *β*-oxidation, depletion of ACC2 gene has been associated with a protective phenotype against obesity and diabetes induced by high-fat/high-carbohydrate diets [66]. Surprisingly, the lack of FAS is not associated with a protective phenotype against dyslipidemia, since it exacerbates the development of fatty diseases by increase malonyl-CoA levels and inhibits *β*-oxidation [66]. Long-chain polyunsaturated fatty acids (PUFA) exhibit strong inhibitory effects on *FAS* and *ACC* [67,68]. However, aligned with our experimental model, it is recognized that the excess of saturated fatty acids (SFA) reduces glucose bioavailability and insulin levels, also attenuating *FAS* and *ACC* gene expression and limiting *de novo* lipogenesis [69]. Although *FAS* and *ACC* modulation by AS

Table 5
Plasmatic levels of triacylglycerol and total cholesterol in control mice and those treated with high-fat diet and anabolic steroid.

Parameters	Triacylglycerol (mg/dL)	Total cholesterol (mg/dL)	HDL cholesterol (mg/dL)	LDL cholesterol (mg/dL)
SD	60.57 ± 5.39^a	169.09 ± 9.50^a	16.85 ± 1.29^a	150.18 ± 9.77^a
SD + AS10	58.21 ± 6.11^a	162.17 ± 8.31^a	16.14 ± 1.33^a	111.37 ± 10.02^b
SD + AS20	60.18 ± 5.33^a	131.85 ± 7.66^b	15.11 ± 1.25^a	100.08 ± 11.58^b
HFD	75.29 ± 5.40^b	170.12 ± 12.64^a	11.26 ± 1.44^b	155.36 ± 12.15^a
HFD + AS10	92.33 ± 7.81^c	165.28 ± 10.44^a	11.09 ± 1.37^b	152.75 ± 9.96^a
HFD + AS20	95.47 ± 6.52^c	160.33 ± 10.01^a	10.40 ± 1.55^b	150.69 ± 10.32^a

SD = standard diet, HFD = high-fat diet, AS10 and 20 = anabolic steroid testosterone cypionate administered at 10 and 20 mg/kg. $^{a, b, c}$Different letters in the columns indicate statistical difference between groups ($P < 0.05$), and groups with the same letter are statistically similar ($P > 0.05$).

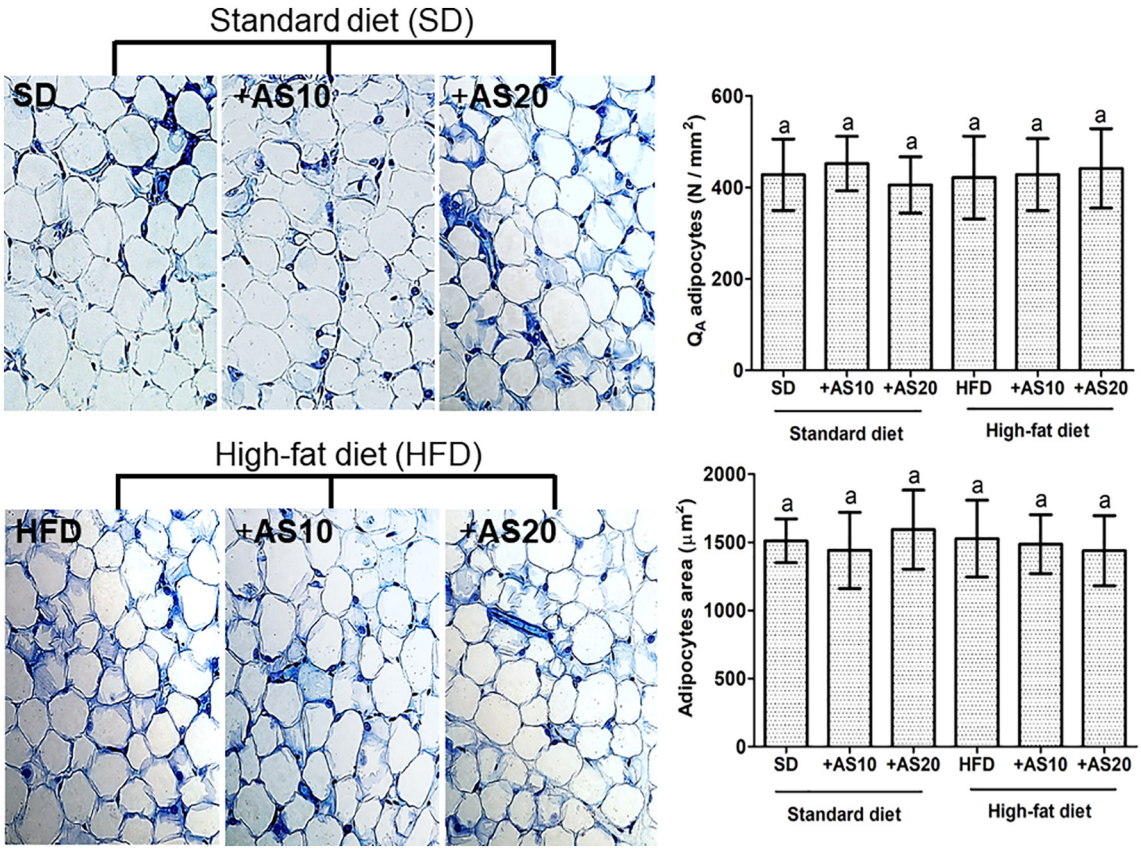

Fig. 6. Number density (Q_A) and mean adipocytes area in control mice and those treated with high-fat diet (HFD) and the anabolic steroid (AS) testosterone cypionate. SD = standard diet, AS10 and 20 = testosterone cypionate administered at 10 and 20 mg/kg. In the graphics, the same letter (a) in the columns indicate that the groups are statistically similar ($P > 0.05$).

are poorly understood, there is evidence that sterols suppress *FAS* expression by a mechanism associated with the inhibition of the transcription factor sterol regulatory element-binding protein 1 (*SREBP-1*) [67].

AS and HFD alone and especially in combination also exerted an interesting effect by inducing UCP-1 upregulation in adipose tissue, indicating a direct modulation on a key component energy metabolism and thermogenesis in adipocytes [70,71]. This effect is potentially related with the activation of an anti-obesogenic mechanism in animals receiving a HFD, which represent an adaptation to limit the increase in adiposity [71], especially considering that uncoupling of oxidative phosphorylation represents up to 50% of all energy expended by the mitochondria in a normal functioning cell [70]. By upregulates of *UCP-1* gene expression, AS also exhibited an anti-obesogenic potential, a proposition reinforced by similar visceral fat mass and adipocytes distribution in animals treated with SD and AS, which also exhibited the highest feed efficiency and final body mass. In these animals, the simultaneous increase in *FAS*, *ACC*, and *UCP-1* expression appears to act as a mechanism that adjusts the balance between lipogenesis and lipolysis, attenuating the accumulation of visceral fat from dietary lipids and those obtained from *de novo* synthesis in AS-treated animals. However, although *FAS* and *ACC* downregulation indicated inhibition of *de novo* synthesis in HFD-treated mice, *UCP-1* upregulation may still be beneficial to assist in the degradation of excess dietary lipids in these animals. In fact, sex hormones such as estradiol, progesterone and testosterone have been associated with an inductive role on *UCP-1* gene and protein, potentiating its responsivity to β-adrenergic stimulation and thermogenesis in adipocytes [72–74]. However, the mechanisms by which steroids hormones modulates lipid metabolism in adipocytes remains poorly understood, especially in the presence of HFD, an issue that requires further investigation.

Taken together, our findings indicated that HFD and AS exerted none or limited effect on body grown and microstructural organization of pancreas, skeletal muscle, and adipose tissue. However, HFD and AS had a profound impact on glycemic control and lipid profile in mice, especially when administered in combination. In general, peripheral insulin sensitivity and glycemic control were improved, while triacylglycerol and LDL cholesterol circulating levels were increased by HFD and AS combination. Due to morphological similarities in pancreatic islets, skeletal muscle, and adipose tissue, divergent profiles of *GCK, Glut-2, Glut-4*, *CPT-1*, *FAS, ACC, and UCP-1* gene expression rather than microstructural changes are suggested as important mediators of AS-induced adaptations in energy metabolism of HFD-treated mice. As our data suggest a disturbing interaction between diet and AS, further studies are necessary and urgent to investigate to what extent this combination may increase the risk of metabolic diseases and death, especially considering that HFD intake and the concomitant use of AS is a potential case of food-drug interaction systematically neglected.

Acknowledgements

This work was supported by the Brazilian agencies: Fundação de Amparo à Pesquisa do Estado de Minas Gerais (FAPEMIG, processes APQ-01895-16 and PPM-00077-18) and Conselho Nacional de Desenvolvimento Científico e Tecnológico (CNPq, processes 303972/2017-3 and 423594/2018-4). This study was financed in part by the Coordenação de Aperfeiçoamento de Pessoal de Nível Superior - Brasil (CAPES) – Finance Code 001. No agency was involved with study design; collection, analysis and interpretation of data; or with the writing and submission of the article.

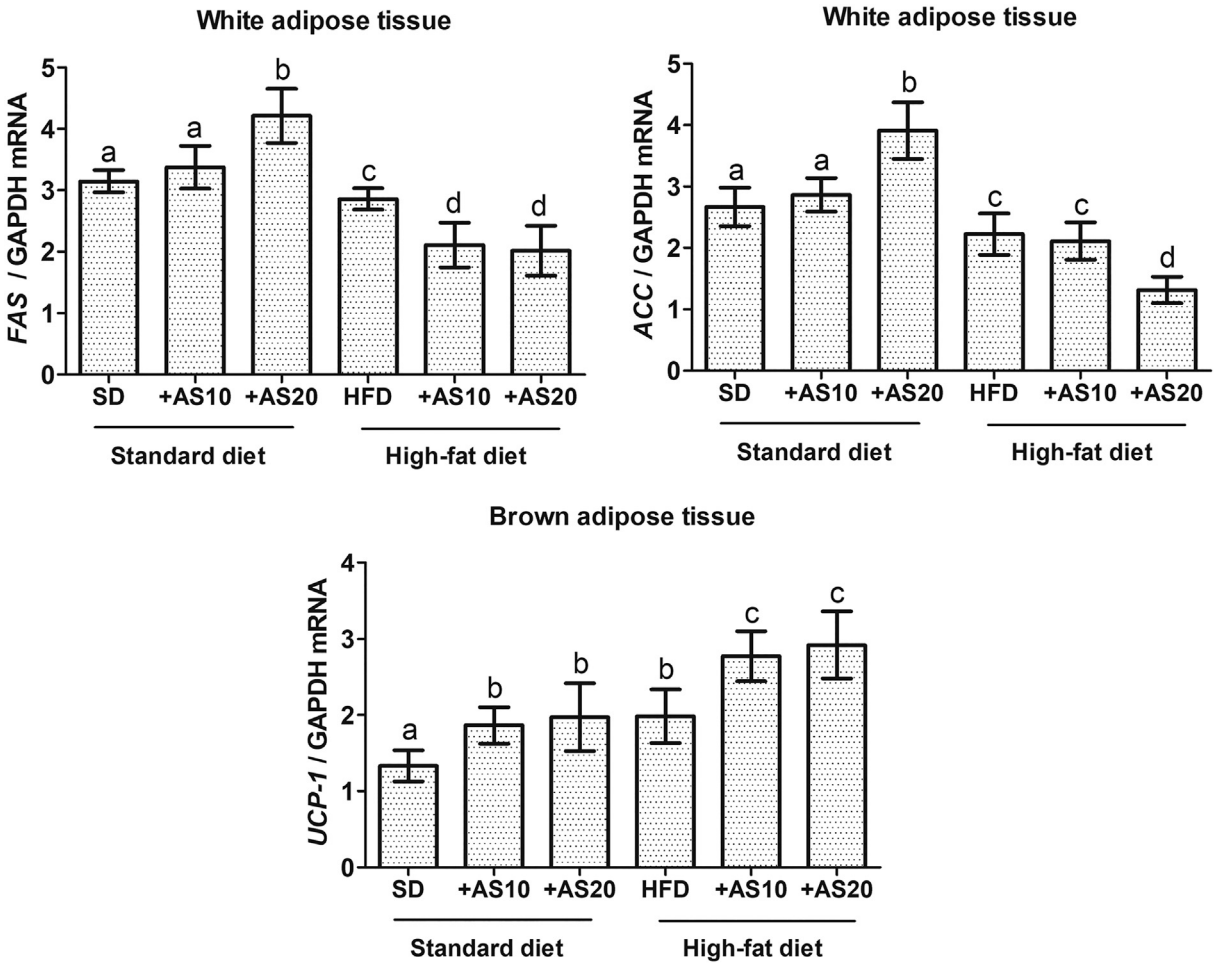

Fig. 7. Gene expression in adipose tissue of mice treated with standard diet (SD) or high-fat diet (HFD) and the anabolic steroid (AS) testosterone cypionate. FAS = fatty acids synthase, ACC = acetyl-CoA carboxylase, UCP-1, uncoupling protein 1, AS10 and 20 = testosterone cypionate administered at 10 and 20 mg/kg. Different letters (a, b, c) in the columns denote statistical differences among the groups ($P < 0.05$), and groups with the same letter are statistically similar ($P > 0.05$).

Conflict of interest

None to declare.

References

[1] R. Chou, et al., Screening for dyslipidemia in younger adults: a systematic review for the U.S. preventive services task force, Ann Int Med 165 (2016) 560–564.
[2] M. Benedict, X. Zhang, Non-alcoholic fatty liver disease: an expanded review, World J. Hepatol. 9 (2017) 715–732.
[3] M.C. Houston, et al., Nonpharmacologic treatment of dyslipidemia, Prog. Cardiovasc. Dis. 52 (2009) 61–94.
[4] A.D. Hendrani, Dyslipidemia management in primary prevention of cardiovascular disease: current guidelines and strategies, World J. Cardiol. 8 (2016) 201–210.
[5] K. Sharma, R.R. Baliga, Genetics of dyslipidemia and ischemic heart disease, Curr. Cardiol. Rep. 19 (2017) 46.
[6] C. Wang, et al., Impact of high-fat diet on liver genes expression profiles in mice model of nonalcoholic fatty liver disease, Env Toxicol Pharmacol 45 (2016) 52–62.
[7] M. Dhibi, et al., The intake of high fat diet with different trans fatty acid levels differentially induces oxidative stress and non alcoholic fatty liver disease (NAFLD) in rats, Nutr Metabol 8 (2011) 65.
[8] H. Xu, L.A. Tartaglia, H. Chen, Chronic inflammation in fat plays a crucial role in the development of obesity-related insulin resistance, J. Clin. Invest. 112 (2003) 1821–1830.
[9] B.P. Sampey, et al., Cafeteria diet is a robust model of human metabolic syndrome with liver and adipose inflammation: comparison to high-fat diet, Obesity 19 (2011) 1109–1117.
[10] M. Carmiel-Haggai, A.I. Cederbaum, N. Nieto, A high-fat diet leads to the progression of non-alcoholic fatty liver disease in obese rats, FASEB J. 19 (2004) 136–138.
[11] D.B. Jump, Dietary polyunsaturated fatty acids and regulation of gene transcription, Curr. Opin. Lipidol. 13 (2002) 155–164.
[12] H. Sampath, J.M. Ntambi, Polyunsaturated fatty acid regulation of gene expression, Nutr. Rev. 62 (2004) 333–339.
[13] G. Baños, V. Guarner, I. Pérez-Torres, Sex steroid hormones, cardiovascular diseases and the metabolic syndrome, Cardiovasc. Hematol. Agents Med. Chem. 9 (2011) 137–146.
[14] G. Baldo-Enzi, et al., Lipid and apoprotein modifications in body builders during and after self-administration of anabolic steroids, Metabolism 39 (1990) 203–208.
[15] V. Guarner-Lans, M.E. Rubio-Ruiz, I. Pérez-Torres, G.B. MacCarthy, Relation of aging and sex hormones to metabolic syndrome and cardiovascular disease, Exp. Gerontol. 46 (2011) 517–523.
[16] S. Basaria, J.T. Wahlstrom, A.S. Dobs, Clinical review 138: anabolic-androgenic steroid therapy in the treatment of chronic diseases, J. Clin. Endocrinol. Metab. 86 (2001) 5108–5117.
[17] C.F. Ebenbichler, et al., Flow-mediated endothelium-dependent vasodilation is impaired in male body builders taking anaboli-androgenic steroids, Atherosclerosis 158 (2001) 483–490.
[18] N.A. Evans, Current concepts in anabolic-androgenic steroids, Am J Sport Med 32 (2004) 534–542.
[19] P.C.A. Kam, M. Yarrow, Anabolic steroid abuse: physiological and anaesthetic considerations, Anaesthesia 60 (2005) 685–692.
[20] G. Glazer, Atherogenic effects of anabolic steroids on serum lipid levels, Arch Int Med 151 (1991) 1925–1933.
[21] J.D.B. Santos, et al., Food-drug interaction: anabolic steroids aggravate hepatic lipotoxicity and nonalcoholic fatty liver disease induced by trans fatty acids, Food Chem. Toxicol. 116 (2018) 360–368.
[22] J. Folch, M. Lees, G.H. Sloane-Stanley, A simple method for the isolation and purification of total lipids from animal tissues, J. Biol. Chem. 226 (1957) 497–509.
[23] L.D. Metcalfe, A.A. Schmitz, J.R. Pelka, Rapid preparation of fatty acid esters from lipids for gas chromatographic analysis, Anal. Chem. 38 (1966) 514–515.
[24] E. Guillocheau, et al., Retroconversion of dietary trans-vaccenic (trans-C18:1 n−7) acid to trans-palmitoleic acid (trans-C16:1 n−7): proof of concept and quantification in both cultured rat hepatocytes and pregnant rats, J. Nutr. Biochem. 63 (2019) 19–26.

[25] J. Molkentin, D. Precht, Determination of trans-octadecenoic acids in German margarines, shortenings, cooking and dietary fats by Ag-TLC/GC, Zeitschrift fur Ernährungswissenschaf 34 (1995) 314–317.
[26] P.L. Sequetto, et al., Low doses of simvastatin potentiate the effect of sodium alendronate in inhibiting bone resorption and restore microstructural and mechanical bone properties in glucocorticoid-induced osteoporosis, Microsc. Microanal. 23 (2017) 989–1001.
[27] P. Pushparaj, C.H. Tan, B.K.H. Tan, Effects of *Averrhoa bilimbi* leaf extract on blood glucose and lipids in streptozotocin-diabetic rats, J. Ethnopharmacol. 72 (2000) 9–76.
[28] R.D. Novaes, et al., *Trypanosoma cruzi* infection alters glucose metabolism at rest and during exercise without modifying the morphology of pancreatic islets in rats, Pathol. Res. Pract. 208 (2012) 480–488.
[29] J.C. Fraulob, et al., A mouse model of metabolic syndrome: insulin resistance, fatty liver and non-alcoholic fatty pancreas disease (NAFPD) in C57BL/6 mice fed a high fat diet, J. Clin. Biochem. Nutr. 46 (2010) 212–223.
[30] R.D. Novaes, et al., Time-dependent resolution of collagen deposition during skin repair in rats: a correlative morphological and biochemical study, Microsc. Microanal. 21 (2015) 1482–1490.
[31] C.M.M. Marques, et al., Beneficial effects of exercise training (treadmill) on insulin resistance and nonalcoholic fatty liver disease in high-fat fed C57Bl/6 mice, Braz. J. Med. Biol. Res. 43 (2010) 467–475.
[32] C.A. Schneider, W.S. Rasband, K.W. Eliceiri, NIH image to ImageJ: 25 years of image analysis, Nat. Methods 9 (2012) 671–675.
[33] J. Jo, Y.M. Choi, D.S. Koh, Size distribution of mouse Langerhans islets, Biophys. J. 93 (2007) 2655–2666.
[34] R.D. Novaes, et al., *Trypanosoma Cruzi* infection induces morphological reorganization of the myocardium parenchyma and stroma, and modifies the mechanical properties of atrial and ventricular cardiomyocytes in rats, Cardiovasc. Pathol. 22 (2013) 270–279.
[35] R.D. Novaes, et al., Nonsteroidal anti-inflammatory is more effective than antioxidant therapy in counteracting oxidative/nitrosative stress and heart disease in *T. Cruzi*-infected mice, Parasitology 144 (2017) 904–916.
[36] R.V. Gonçalves, et al., Hepatoprotective effect of Bathysa cuspidata in a murine model of severe toxic liver injury, Internat J Exp Pathol 93 (2012) 370–376.
[37] A. Yessoufou, K. Moutairou, N.A. Khan, A model of insulin resistance in mice, born to diabetic pregnancy, is associated with alterations of transcription-related genes in pancreas and epididymal adipose tissue, J. Obes. 2011 (2011) 654967.
[38] J.M. Gurley, B.A. Griesel, A.L. Olson, Increased skeletal muscle GLUT4 expression in obese mice after voluntary wheel running exercise is posttranscriptional, Diabetes 65 (2016) 2911–2919.
[39] C. Hénique, et al., Increasing mitochondrial muscle fatty acid oxidation induces skeletal muscle remodeling toward an oxidative phenotype, FASEB J. 29 (2015) 2473–2483.
[40] K. Morgan, et al., Altered expression of transcription factors and genes regulating lipogenesis in liver and adipose tissue of mice with high fat diet-induced obesity and nonalcoholic fatty liver disease, Eur. J. Gastroenterol. Hepatol. 20 (2008) 843–854.
[41] C. Sun, Z.W. Wei, Y. Li, DHA regulates lipogenesis and lipolysis genes in mice adipose and liver, Molecul Bioly Rep 38 (2011) 731–737.
[42] P. Christian, C.P. Stewart, Maternal micronutrient deficiency, fetal development, and the risk of chronic disease, J. Nutr. 140 (2010) 437–445.
[43] A.R. Penitente, et al., Protein restriction after weaning modifies the calcium kinetics and induces cardiomyocyte contractile dysfunction in rats, Cell Tissue Org 198 (2013) 311–317.
[44] R.C. Griggs, et al., Effect of testosterone on muscle mass and muscle protein synthesis, J. Appl. Physiol. 66 (1989) 498–503.
[45] E.A. Richter, M. Hargreaves, Exercise, GLUT4, and skeletal muscle glucose uptake, Physiol. Rev. 93 (2013) 993–1017.
[46] A. Zorzano, M. Palacín, A. Gumà, Mechanisms regulating GLUT4 glucose transporter expression and glucose transport in skeletal muscle, Acta Physiol. Scand. 183 (2005) 43–58.
[47] B.B. Rasmussen, et al., Malonyl coenzyme A and the regulation of functional carnitine palmitoyltransferase-1 activity and fat oxidation in human skeletal muscle, J. Clin. Invest. 110 (2002) 1687–1693.
[48] R.L. Dobbins, et al., Prolonged inhibition of muscle carnitine lipid accumulation and insulin resistance in rats, Diabetes 50 (2001) 123–130.
[49] L.A. Brondani, et al., The role of the uncoupling protein 1 (UCP1) on the development of obesity and type 2 diabetes mellitus, Arqs Bras Endocrinol Metabol 56 (2012) 215–225.
[50] M. Chondronikola, et al., Brown adipose tissue improves whole-body glucose homeostasis and insulin sensitivity in humans, Diabetes 63 (2014) 4089–4099.
[51] F.C. Schuit, Is GLUT2 required for glucose sensing? Diabetologia 40 (1997) 104–111.
[52] B. Thorens, GLUT2, glucose sensing and glucose homeostasis, Diabetologia 58 (2014) 221–232.
[53] Y. Kim, et al., Effect of high-fat diet on the gene expression of pancreatic GLUT2 and glucokinase in rats, Biochem. Biophys. Res. Commun. 208 (1995) 1092–1098.
[54] M.K. Reimer, B. Ahren, Altered β-cell distribution of Pdx-1 and GLUT-2 after a short-term challenge with a high-fat diet in C57BL/6J mice, Diabetes 51 (2002) 138–143.
[55] M.S. Winzell, C. Magnusson, B. Ahrén, Temporal and dietary fat content-dependent islet adaptation to high-fat feeding-induced glucose intolerance in mice, Metabol Clin Exp 56 (2007) 122–128.
[56] A.R. Kennedy, et al., A high-fat, ketogenic diet induces a unique metabolic state in mice, Am J Physiol Endocrinol Metabol 292 (2007) 1724–1739.
[57] J. Kim, et al., Improved glucose tolerance with restored expression of glucose transporter 4 in C57BL/6 mice after a long period of high-fat diet feeding, An Cell Syst 18 (2014) 197–203.
[58] G.W. Power, E.A. Newsholme, Dietary fatty acids influence the activity and metabolic control of mitochondrial carnitine palmitoyltransferase I in rat heart and skeletal muscle, J. Nutr. 127 (1997) 2142–2150.
[59] M. Collino, et al., Variability in myosteatosis and insulin resistance induced by high-fat diet in mouse skeletal muscles, BioMed Res Internat 2014 (2014) 569623.
[60] C. Wilson, et al., Testosterone increases GLUT4-dependent glucose uptake in cardiomyocytes, J. Cell. Physiol. 228 (2013) 2399–2407.
[61] S. Morimoto, F. Jiménez-Trejo, M. Cerbón, Sex steroids effects in normal endocrine pancreatic function and diabetes, Curr Topic Med Chem 11 (2011) 1–8.
[62] C. Le May, et al., Estrogens protect pancreatic beta-cells from apoptosis and prevent insulin-deficient diabetes mellitus in mice, Proc Nat Acad Sci 103 (2006) 9232–9237.
[63] G. Navarro, et al., Extranuclear actions of the androgen receptor enhance glucose-stimulated insulin secretion in the male, Cell Metabol 23 (2016) 837–851.
[64] M.C. Medina, et al., Dehydroepiandrosterone increases β-cell mass and improves the glucose-induced insulin secretion by pancreatic islets from aged rats, FEBS Lett. 580 (2006) 285–290.
[65] H. Liu, et al., Testosterone improves the differentiation efficiency of insulin-producing cells from human induced pluripotent stem cells, PLoS One 12 (2017) 1–11.
[66] C. Postic, J. Girard, Contribuition of de novofatty acidsynthesis to hepatic steatosis and insulinresistance: lessons from genetically engineered mice, J. Clin. Invest. 118 (2008) 829–838.
[67] C.F. Semenkovich, Regulation of fatty acid synthase (FAS), Prog. Lipid Res. 36 (1997) 43–53.
[68] K. Musch, M.A. Ojakian, M.A. Williams, Comparison of α-linolenate and oleate in lowering activity of lipogenic enzymes in rat liver: evidence for a greater effect of dietary linolenate independent of food and carbohydrate intake, Biochim. Biophys. Acta 337 (1974) 343–348.
[69] J.D. Paulauskis, H.S. Sul, Hormonal regulation of mouse fatty acid synthase gene transcription in liver, J. Biol. Chem. 264 (1989) 574–577.
[70] P.P. Argentato, H. de Cássia César, D. Estadella, L.P. Pisani, Programming mediated by fatty acids affects uncoupling protein 1 (UCP-1) in brown adipose tissue, Br. J. Nutr. 120 (2018) 619–627.
[71] E. García-Ruiz, et al., The intake of high-fat diets induces the acquisition of brown adipocyte gene expression features in white adipose tissue, Int. J. Obes. 39 (2015) 1619–1629.
[72] C. Quarta, R. Mazza, R. Pasquali, U. Pagotto, Role of sex hormones in modulation of brown adipose tissue activity, J. Mol. Endocrinol. 49 (2012) 1–7.
[73] S. Rodríguez-Cuenca, et al., Expression of mitochondrial biogenesis-signaling factors in brown adipocytes is influenced specifically by 17β-estradiol, testosterone, and progesterone, Am J Physiol Endocrinol Metabol 292 (2007) E340–E346.
[74] M. Suzuki, et al., Role of estradiol and testosterone in Ucp1 expression in brown/beige adipocytes, Cell Biochem Func 36 (2018) 450–456.